

# Dissociation of Antimicrobial and Hemolytic Activities in Cyclic Peptide Diastereomers by Systematic Alterations in Amphipathicity\*

(Received for publication, December 1, 1998, and in revised form, February 20, 1999)

Leslie H. Kondejewski<sup>‡</sup>, Masood Jelokhani-Niaraki<sup>‡</sup>, Susan W. Farmer<sup>§</sup>, Bruce Lix<sup>‡</sup>,  
Cyril M. Kay<sup>‡¶</sup>, Brian D. Sykes<sup>‡¶</sup>, Robert E. W. Hancock<sup>§</sup>, and Robert S. Hodges<sup>‡¶||</sup>

From the <sup>‡</sup>Protein Engineering Network of Centres of Excellence and <sup>¶</sup>Department of Biochemistry, University of Alberta, Edmonton, Alberta T6G 2S2, Canada and the <sup>§</sup>Department of Microbiology and the Canadian Bacterial Diseases Network, University of British Columbia, Vancouver, British Columbia V6T 1Z3, Canada

We have investigated the role of amphipathicity in a homologous series of head-to-tail cyclic antimicrobial peptides in efforts to delineate features resulting in high antimicrobial activity coupled with low hemolytic activity (*i.e.* a high therapeutic index). The peptide GS14, cyclo(VKLKVD-YPLKVKLD-YP), designed on the basis of gramicidin S (GS), exists in a preformed highly amphipathic  $\beta$ -sheet conformation and was used as the base compound for this study. Fourteen diastereomers of GS14 were synthesized; each contained a different single enantiomeric substitution within the framework of GS14. The  $\beta$ -sheet structure of all GS14 diastereomers was disrupted as determined by CD and NMR spectroscopy under aqueous conditions; however, all diastereomers exhibited differential structure inducibility in hydrophobic environments. Because the diastereomers all have the same composition, sequence, and intrinsic hydrophobicity, the amphipathicity of the diastereomers could be ranked based upon retention time from reversed-phase high performance liquid chromatography. There was a clear correlation showing that high amphipathicity resulted in high hemolytic activity and low antimicrobial activity in the diastereomers. The latter may be the result of increased affinity of highly amphipathic peptides to outer membrane components of Gram-negative microorganisms. The diastereomers possessing the most favorable therapeutic indices possessed some of the lowest amphipathicities, although there was a threshold value below which antimicrobial activity decreased. The best diastereomer exhibited 130-fold less hemolytic activity compared with GS14, as well as greatly increased antimicrobial activities, resulting in improvement in therapeutic indices of between 1,000- and 10,000-fold for a number of microorganisms. The therapeutic indices of this peptide were between 16- and 32-fold greater than GS for Gram-negative microorganisms and represents a significant improvement in specificity over GS. Our findings show that a highly amphipathic nature is not desirable in the design of constrained cyclic antimicrobial peptides and that an optimum amphipathicity can be defined by systematic enantiomeric substitutions.

The ever-increasing development of bacterial resistance to traditional antibiotics has reached alarming levels, making it essential that new antibiotics be developed (1). Ideally, these new antibiotics should possess both novel modes of action as well as different cellular targets compared with existing antibiotics to decrease the likelihood of development of cross-resistance. Antimicrobial peptides may represent such a new class of antibiotics, and their design and structure-activity relationships have become an area of active research in recent years (see Refs. 2 and 3 and references therein). Although their exact mode of action has not been established, it has been proposed that the cytoplasmic membrane is the main target of these peptides, where their accumulation results in increased permeability and loss of barrier function. The development of resistance to these membrane active peptides is not expected because this would require substantial changes in the lipid composition of cell membranes. Indeed, the induction of resistance to such peptides has not been seen for a number of the antimicrobial peptides (2). Because both their mode of action and cellular targets are different from those of the traditional antibiotics, antimicrobial peptides represent a truly new class of antibiotics and are therefore attractive candidates for development as such.

Two major classes of the cationic antimicrobial peptides are the  $\alpha$ -helical and the  $\beta$ -sheet peptides. The  $\alpha$ -helical class (for example cecropins, magainins, and melittin) are linear peptides that exist as disordered structures in aqueous media and become helical upon interaction with hydrophobic solvents or phospholipid vesicles. Unlike the  $\alpha$ -helical peptides,  $\beta$ -sheet peptides are cyclic peptides constrained in this conformation either by disulfide bonds (tachyplesins, protegrins, and polyphemusins) or by cyclization of the backbone (gramicidin S and tyrocidines). Although the  $\beta$ -sheet conformations of these peptides may be further stabilized in the presence of a hydrophobic or lipid environment, they exist largely in a "preformed"  $\beta$ -sheet conformation in aqueous environments due to their structural constraints. From numerous structure-activity studies on both natural and synthetic antimicrobial peptides, a number of factors believed to be important for antimicrobial activity have been identified. These include the presence of both hydrophobic and basic residues, as well as a defined secondary structure ( $\alpha$ -helical or  $\beta$ -sheet), either preformed or inducible, and an amphipathic nature that segregates basic and hydrophobic residues to opposite sides of the molecule in lipid or lipid-mimicking environments (2–5).

Many of the antimicrobial peptides show poor selectivity for bacteria in that they are also toxic to higher eukaryotic cells. To make the antimicrobial peptides useful as therapeutics therefore requires delineation of the features responsible for antimi-

\* This study was supported by the Canadian Government through grants to the Canadian Bacterial Diseases Network (to R. E. W. H.) and the Protein Engineering Network of Centers of Excellence (to R. S. H.). The costs of publication of this article were defrayed in part by the payment of page charges. This article must therefore be hereby marked "advertisement" in accordance with 18 U.S.C. Section 1734 solely to indicate this fact.

|| To whom correspondence should be addressed. Tel.: 780-492-2758; Fax: 780-492-1473; E-mail: robert.hodges@ualberta.ca.

robial activity from those responsible for toxicity to higher eukaryotic cells (typically measured as hemolytic activity). The obvious goal is to design peptides that have high antimicrobial activity coupled with low toxicity, *i.e.* a high specificity or high therapeutic index. Recent studies on a number of linear peptides have attempted to delineate features responsible for these activities and found that high amphipathicity (6, 7), high hydrophobicity (6, 8), as well as high helicity (9, 10) were correlated with increased hemolytic activity. Antimicrobial activity on the other hand was found to be less dependent on peptide helicity (9, 10). Furthermore, decreases in either hydrophobicity or amphipathicity were either found to increase (7, 8) or to decrease antimicrobial activity (6, 11), depending on the peptides studied. In both cases, however, specificity for bacteria over erythrocytes could be increased either by increasing activity coupled with decreased hemolysis (7, 8) or because the hemolytic activity was decreased more readily than antimicrobial activity (6, 11).

Relatively few studies have investigated structural features responsible for the hemolytic and antimicrobial properties of the cyclic  $\beta$ -sheet peptides. The fact that these peptides are constrained and therefore have less conformational freedom compared with the linear  $\alpha$ -helical peptides suggests that the properties of these peptides may be different. We have utilized the 10 residue head-to-tail cyclic peptide gramicidin S (GS)<sup>1</sup> (12) as the basis of our design for novel antimicrobial agents. GS has the sequence cyclo(Val-Orn-Leu-*d*-Phe-Pro)<sub>2</sub> and exists in an antiparallel  $\beta$ -sheet conformation with the strands fixed in place by two type II'  $\beta$ -turns (5, 13, 14). The  $\beta$ -sheet structure gives the molecule a preformed amphipathic nature with four hydrophobic residues (Val and Leu) making up one face of the molecule and two basic Orn residues making up the other face. This amphipathicity, along with high hydrophobicity, has long been thought to be important for the antimicrobial properties of GS-like peptides (5, 15–18). A previous study with cyclic  $\beta$ -sheet antimicrobial peptides based on GS indicated that it is possible to dissociate antimicrobial and hemolytic activities through gross manipulation of  $\beta$ -sheet structure and amphipathicity (19). In this manuscript, we report on the effect of small incremental changes in amphipathicity (directed hydrophobicity and positive charge) on the antimicrobial and hemolytic properties of cyclic 14 residue peptides. We have utilized the cyclic tetradecapeptide, GS14, cyclo(VKLKVD-YPLKVKLd-YP), as the model peptide in this study. This peptide has been shown to exist in a highly amphipathic  $\beta$ -sheet structure, with six hydrophobic residues on one face of the molecule and four basic residues on the opposite face (19, 20). Unlike GS, which exhibits broad spectrum antimicrobial activity as well as hemolytic activity, GS14 was found to possess limited antimicrobial activity and very high hemolytic activity (19). Because amphipathicity is intimately linked to  $\beta$ -sheet structure in GS14, any change in  $\beta$ -sheet structure was predicted to directly affect the amphipathicity of the molecule. We have created a series of GS14 diastereomers in which each contains a different single residue enantiomeric substitution within the framework of GS14 resulting in a series of cyclic peptides possessing graded disruption of  $\beta$ -sheet structure and amphipathicity. The present method of enantiomeric substitutions within a constrained backbone system has the advantage that all peptides retain the same sequence, intrinsic hydrophobicity, and basicity but differ only in structure. We

show that the amphipathicity of these peptides has a large effect on their biological properties and that by defining the optimum amphipathicity in the framework of these cyclic peptides, the balance between hemolytic and antimicrobial activities can be optimized.

#### MATERIALS AND METHODS

**Peptide Synthesis, Purification, and Cyclization**—All peptides were synthesized by solid phase peptide synthesis using standard *t*-butyloxycarbonyl chemistry, cleaved from the resin, and purified by preparative RP-HPLC as reported previously (19). For all peptides proline was the C terminus because racemization can occur during the cyclization reaction with other residues.<sup>2</sup> Purity of linear peptides was verified by analytical RP-HPLC, and correct peptide masses were verified by electrospray mass spectrometry on a Fisons VG Quattro triple quadrupole mass spectrometer (Manchester, UK). Pure linear side chain protected peptides were cyclized, deprotected, and purified by preparative RP-HPLC as described (19). Purified cyclic peptides were homogeneous by analytical RP-HPLC and gave correct primary ion molecular weights by mass spectrometry as well as appropriate amino acid analysis ratios. Peptide concentrations of stock solutions were determined by amino acid analysis for subsequent use in biological assays.

**Analytical Reversed-phase Analysis of Diastereomers**—Peptides were analyzed by RP-HPLC on a Zorbax SB-C8 column (150 × 2.1-mm inner diameter, 5  $\mu$ m particle size, 300 Å pore size; Rockland Technologies, Wilmington, DE) using a Hewlett Packard 1100 chromatograph at 70 °C with a linear AB gradient of 1% B/min (where solvent A was 0.5% aqueous trifluoroacetic acid and solvent B was 0.5% trifluoroacetic acid in acetonitrile) at a flow rate of 0.25 mL/min.

**Circular Dichroism Measurements**—CD spectra were recorded on a Jasco J-500C spectropolarimeter (Jasco, Easton, MD) as described (19). Spectra were recorded in either 5 mM sodium acetate buffer, pH 5.5, or 5 mM sodium acetate buffer, pH 5.5, containing 50% trifluoroethanol (TFE).

**NMR Spectroscopy**—NMR spectroscopy was carried out under aqueous conditions on a Varian Unity 300 MHz spectrometer equipped with a 5-mm inverse detection probe. Each peptide was dissolved in 500  $\mu$ l of 90% H<sub>2</sub>O/10% D<sub>2</sub>O (or 100% D<sub>2</sub>O) giving a sample concentration of 1–2 mM, and the pH was adjusted to 5.5. <sup>1</sup>H double quantum filtered two-dimensional correlated spectroscopy, rotating frame Overhauser effect spectroscopy, and total correlation spectroscopy spectra were collected at 25 °C and processed as described (21). The chemical shift index was calculated for selected peptides as described by Wishart *et al.* (22).

**Molecular Modelling**—A model of GS14 was constructed using Insight II (Biosym Technologies Inc., San Diego, CA) on a Silicon Graphics workstation starting with the linear peptide LKVD-YPLKVKLd-YPVK. The model was constructed by specifying standard antiparallel  $\beta$ -sheet  $\phi$ ,  $\psi$  values of  $-139^\circ$  and  $+135^\circ$ , respectively (23). Two type II'  $\beta$ -turns were incorporated into the model designating D-Tyr and Pro residues as residues *i* + 1 and *i* + 2 of the turns. Dihedral angles ( $\phi$ ,  $\psi$ ) used for the turns were  $60^\circ$ ,  $-120^\circ$  and  $-80^\circ$ ,  $0^\circ$  for *i* + 1 and *i* + 2 residues, respectively (23). The formation of the turns brought the N and C termini into close proximity, and an amide bond was formed between the termini. The model was subjected to energy minimization using the consistent valence force field (24) with a distance-dependent dielectric constant of 4 at pH 7 with no cross-terms. The potential energy of the model was minimized in two steps, first using the steepest descent algorithm for 100 iterations followed by 100 iterations using the VA09A algorithm.

**Calculation of Peptide Hydrophobic Moment and Hydrophobicity**—The mean residue hydrophobic moment ( $\mu$ ) of GS14 and a comparable linear  $\alpha$ -helical peptide (7) was calculated using the consensus hydrophobicity scale of Eisenberg *et al.* (25) to facilitate comparison with other antimicrobial peptides. Due to the cyclic nature of GS14, calculation of  $\mu$  was carried out for each half of the molecule, and the value reported represented the average of these values. This procedure was necessary to account for the two  $\beta$ -turns in the molecule and appears to be a reasonable assumption based on the molecular model. The two segments used for the calculations were: VKLKVYP and LKVKLYP; a value of  $\delta = 180^\circ$  was used for the angle at which successive side chains emerge from the backbone of the  $\beta$ -sheet.

**Measurement of Antibacterial, Antifungal, and Hemolytic Activity**—Minimal inhibitory concentrations (MICs) were measured using a

<sup>1</sup> The abbreviations used are: GS, gramicidin S; LPS, lipopolysaccharide; MIC, minimal inhibitory concentration; NPN, 1-N-phenyl-naphthylamine; RP-HPLC, reversed-phase high performance liquid chromatography; TFE, trifluoroethanol; dansyl, 5-dimethylamino-naphthalene-1-sulfonyl.

<sup>2</sup> L. H. Kondejewski and R. S. Hodges, unpublished results.

TABLE I  
Sequences and biological and physical properties of GS14 diastereomers

Peptide name	Linear sequence <sup>a</sup>	Retention time <sup>b</sup>	LPS binding affinity <sup>c</sup>	Hemolytic activity <sup>d</sup>
		min	$\mu\text{M}$	$\mu\text{g/ml}$
GS	VOL <u>F</u> PVOL <u>F</u> P	54.9	295	12.5
GS14	VKLK <u>V</u> YPLK <u>V</u> KLYP	50.6	3	1.5
GS14V10	VKLK <u>V</u> YPLK <u>V</u> KLYP	45.4	18	6.2
GS14L3	VKLK <u>V</u> YPLK <u>V</u> KLYP	44.2	35	12.5
GS14P14	VKLK <u>V</u> YPLK <u>V</u> KLYP	42.9	20	6.2
GS14P7	VKLK <u>V</u> YPLK <u>V</u> KLYP	42.6	18	12.5
GS14V1	VKLK <u>V</u> YPLK <u>V</u> KLYP	41.3	41	40
GS14L12	VKLK <u>V</u> YPLK <u>V</u> KLYP	41.3	32	25
GS14V5	VKLK <u>V</u> YPLK <u>V</u> KLYP	41.1	33	150
GS14Y13	VKLK <u>V</u> YPLK <u>V</u> KLYP	40.6	24	12.5
GS14L8	VKLK <u>V</u> YPLK <u>V</u> KLYP	40.3	62	50
GS14Y6	VKLK <u>V</u> YPLK <u>V</u> KLYP	40.2	20	25
GS14K2	VKLK <u>V</u> YPLK <u>V</u> KLYP	39.8	50	50
GS14K9	VKLK <u>V</u> YPLK <u>V</u> KLYP	38.8	60	100
GS14K4	VKLK <u>V</u> YPLK <u>V</u> KLYP	37.8	93	200
GS14K11	VKLK <u>V</u> YPLK <u>V</u> KLYP	37.1	50	150
GS14K2K4	VKLK <u>V</u> YPLK <u>V</u> KLYP	33.1	120	>200
GS14K2K4K9K11	VKLK <u>V</u> YPLK <u>V</u> KLYP	28.5	200	>200

<sup>a</sup> Linear sequences of cyclic peptides. Underlined residues represent D-amino acids. O is ornithine.

<sup>b</sup> Retention time on RP-HPLC as determined from Fig. 6.

<sup>c</sup> Peptide concentration to displace 50% of dansyl-polymyxin B from LPS as described under "Materials and Methods."

<sup>d</sup> Peptide concentration required for 100% lysis of human erythrocytes.

standard microtitre dilution method in Luria Broth no salt medium utilizing the same bacterial strains as reported (19). MICs were determined as the lowest peptide concentration that inhibited growth after 24 h at 37 °C. The hemolytic activity of peptides was measured in saline utilizing human erythrocytes as described (16, 19). The concentration of peptide required for complete hemolysis was determined visually after 24 h at 37 °C.

**Measurement of Peptide Outer Membrane Interactions**—Dansyl-polymyxin B displacement from *Pseudomonas aeruginosa* lipopolysaccharide (LPS) was measured to determine the binding affinity of the peptides to LPS (19). Permeabilization of bacterial outer membranes was measured by monitoring peptide mediated 1-N-phenylanthalamine (NPN) fluorescence increases utilizing *Escherichia coli* UB1005 cells (16, 19).

## RESULTS

### Design of Cyclic Peptides

In this study we systematically replaced each residue in the sequence of the highly amphipathic  $\beta$ -sheet peptide, GS14, with its enantiomer (Table I). The rationale for these substitutions was based on the following observations: (a) In a previous study (19) we found that with certain cyclic peptides the lack of  $\beta$ -sheet structure and amphipathicity under aqueous conditions was the key to achieving a high specificity for microbes over human erythrocytes (*i.e.* a high therapeutic index). In that study, the disruption of  $\beta$ -sheet structure and amphipathicity was accomplished by utilizing peptides that could not form  $\beta$ -sheet structures due to the number of residues in the ring (19, 20). (b) During the initial synthesis and cyclization of GS14 we found that racemization of the C terminus could occur during the cyclization reaction when the C terminus was a non-Pro residue and that this racemization led to loss of  $\beta$ -sheet structure.<sup>2</sup> Together, these observations led us to hypothesize that GS14 could be transformed into a peptide possessing a high therapeutic index by disrupting the  $\beta$ -sheet character, and hence the amphipathicity, of the molecule. To accomplish this, we synthesized all 14 possible diastereomers of GS14; each contains a different single amino acid enantiomeric substitution. We also synthesized two diastereomers with two and four enantiomeric substitutions, respectively (Table I). The peptides were characterized with respect to their structural and biological properties.

### Structure of GS14 Diastereomers

**Circular Dichroism Spectroscopy**—The CD spectra of GS14 and representative single residue substitution diastereomers under aqueous conditions are shown in Fig. 1A. It has been shown by NMR spectroscopy that both GS and GS14 possess a similar  $\beta$ -sheet conformation and that they also exhibit similar CD spectra with large negative ellipticities at 206 and 223 nm (19, 20), reminiscent of a combination of  $\beta$ -sheet structure and type II  $\beta$ -turns (26). All of the single replacement diastereomers as well as those containing two or four enantiomeric substitutions exhibited CD spectra more typical of disordered structures, indicating that enantiomeric substitutions within the framework of GS14 resulted in the disruption of  $\beta$ -sheet structure. The CD spectra of GS14 and representative diastereomers recorded in the presence of the lipid-mimicking solvent, TFE, are shown in Fig. 1B. TFE is generally thought of as a helix-inducing solvent (see Ref. 27 and references therein); however, recent studies have shown that aqueous solutions containing TFE can also stabilize  $\beta$ -hairpin and  $\beta$ -turn structures (28, 29). In 50% TFE the molar ellipticities around 206 and 223 nm were significantly enhanced for GS14 as well as all the diastereomers, suggesting an enhancement or stabilization of  $\beta$ -sheet structure in the peptides. However, because the shape of the observed CD spectra of these cyclic peptides is a combination of contributions by  $\beta$ -turns, aromatic residues, and  $\beta$ -sheet structure, it is difficult to assign particular secondary structural elements to these spectra (26). One striking difference in the CD spectra of all diastereomers in the presence of TFE was displayed by GS14K4 (and GS14K11; not shown), with a large blue-shifted negative ellipticity in the vicinity of 200 nm when compared with all other diastereomers (Fig. 1B). This large increase in molar ellipticity at 205 nm for GS14K4 and GS14K11 is also evident from Fig. 2, where molar ellipticity changes in the different environments at both 205 and 220 nm are summarized graphically. The majority of peptides exhibited greater negative molar ellipticities at both these wavelengths in the presence of TFE. It is noteworthy, however, that although all diastereomers exhibited essentially identical spectra under aqueous conditions, all displayed considerably

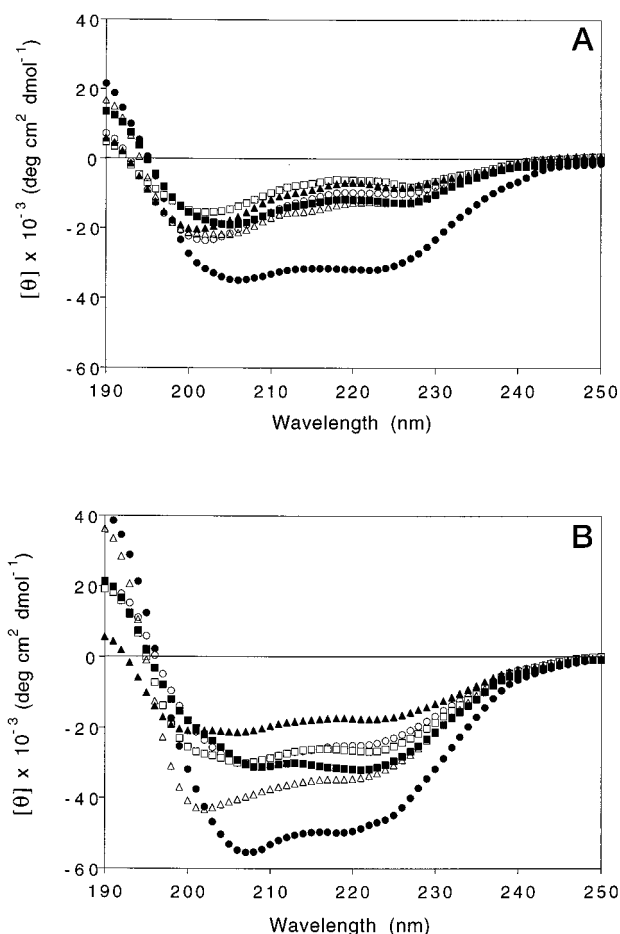


FIG. 1. CD spectra of GS14 and representative GS14 diastereomers. A, spectra were recorded in 5 mM sodium acetate buffer, pH 5.5, at 20 °C at a peptide concentration of approximately 0.3 mM. Samples were GS14 (●), GS14V1 (○), GS14K2 (□), GS14L3 (■), GS14K4 (△), and GS14V5 (▲). B, spectra were recorded in 5 mM sodium acetate buffer, pH 5.5, containing 50% TFE, at 20 °C. Samples were as in A.

different CD spectra in TFE, indicating the induction of different backbone conformations in a hydrophobic environment, depending on the position of the enantiomeric substitution. The diastereomers also displayed similar structural changes in the presence of either SDS micelles or phospholipid vesicles (data not shown).

**NMR Spectroscopy**—The extent of disruption of the  $\beta$ -sheet structure in the GS14 diastereomers was confirmed/demonstrated by NMR spectroscopy for selected analogs.<sup>3</sup> The regions of the <sup>1</sup>H NMR spectrum containing the amide and aromatic proton resonances are shown in Fig. 3 for GS14 (*top spectrum*) and one diastereomer, GS14K2 (*bottom spectrum*). The GS14 spectrum showed 12 well resolved amide resonances (each is a doublet corresponding to the amide resonances of Val<sup>1</sup> to Tyr<sup>6</sup> and Leu<sup>8</sup> to Tyr<sup>13</sup>), and a single pair of doublets corresponding to the meta (2,6) and ortho (3,5) protons of both Tyr<sup>6</sup> and Tyr<sup>13</sup>. The diverse chemical shifts for the amide resonances indicate a well ordered structure, and the downfield chemical shifts indicate significant  $\beta$ -sheet structure. The single pair of doublets for Tyr<sup>6</sup> and Tyr<sup>13</sup> indicates that both are in equivalent environments. By comparison, the amide resonances observed for GS14K2 were much less diverse and centered more around the random coil value, indicating disruption of  $\beta$ -sheet structure.

<sup>3</sup> The complete <sup>1</sup>H NMR assignments for these analogs are available at <http://www.pence.ualberta.ca/ftp/kondejewski.html>.

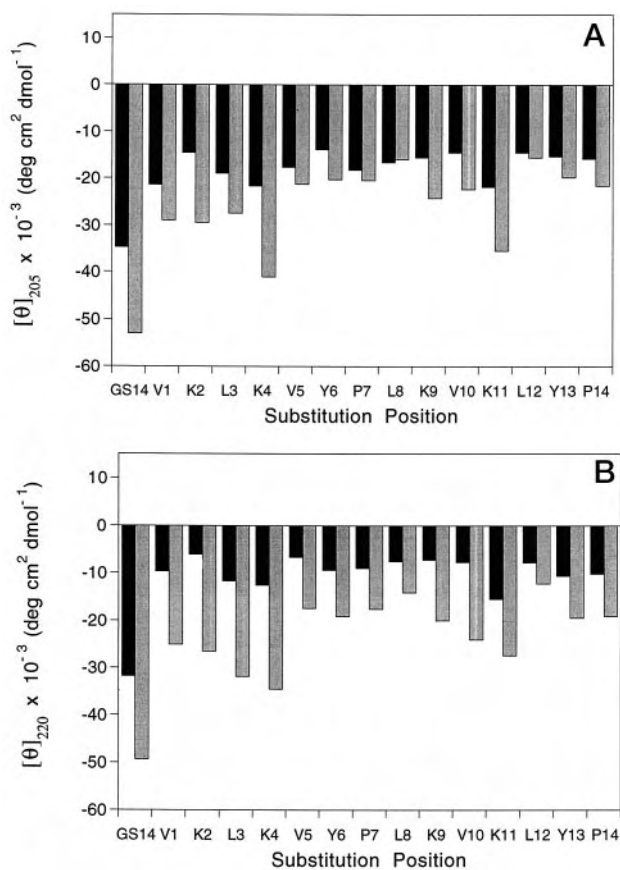


FIG. 2. Environment-dependent CD spectral changes in GS14 diastereomers. Molar ellipticities at 205 (A) and 220 nm (B) are shown for the diastereomers under aqueous conditions (*black bars*) and in the presence of 50% TFE (*gray bars*).

In addition, two pairs of doublets were observed for Tyr<sup>6</sup> and Tyr<sup>13</sup>, indicating that they are not equivalent in the structure. The  $H_{\alpha}$  chemical shift deviations from random coil values for GS14 and three diastereomers are shown in Fig. 4. Positive chemical shift deviations greater than 0.1 ppm indicate downfield shifted resonances relative to random coil values, and a cluster of three or more continuous positive chemical shifts is indicative of  $\beta$ -sheet structure (22). It is apparent that the  $H_{\alpha}$  chemical shifts for GS14 (Fig. 4A) were all  $\beta$ -sheet-like within the  $\beta$ -strands of the molecule (see molecular model below) and non- $\beta$ -sheet chemical shifts in the turns defined by the D-Tyr-Pro sequence. It is clear from the chemical shift analysis of representative diastereomers (Fig. 4, B, C, and D) that the strands contained less  $\beta$ -sheet structure and the turns became more disrupted compared with GS14. It is also noteworthy that the three diastereomers differed in both the extent and location of disruption, indicating that they were structurally different under aqueous conditions.

**Molecular Model of GS14**—Both CD and NMR spectroscopy indicated that GS14 possesses a  $\beta$ -sheet structure similar to GS. A model of GS14 was constructed to contain the essential features as present in GS, namely, an antiparallel  $\beta$ -sheet structure with two type II'  $\beta$ -turns defined by the D-Tyr-Pro sequence. As shown in Fig. 5, the incorporation of both the cyclic constraint (due to backbone cyclization of the peptide) as well as secondary structural constraints ( $\beta$ -sheet and turns) results in a highly amphipathic molecule where Val and Leu residues make up the hydrophobic face and Lys residues make up the basic face of the molecule (Fig. 5, *lower panel*). There are

FIG. 3. One-dimensional  $^1\text{H}$  NMR spectra of the amide regions for GS14 and GS14K2. Spectra were recorded in  $\text{H}_2\text{O}$ , pH 5.5, at 20  $^\circ\text{C}$ .

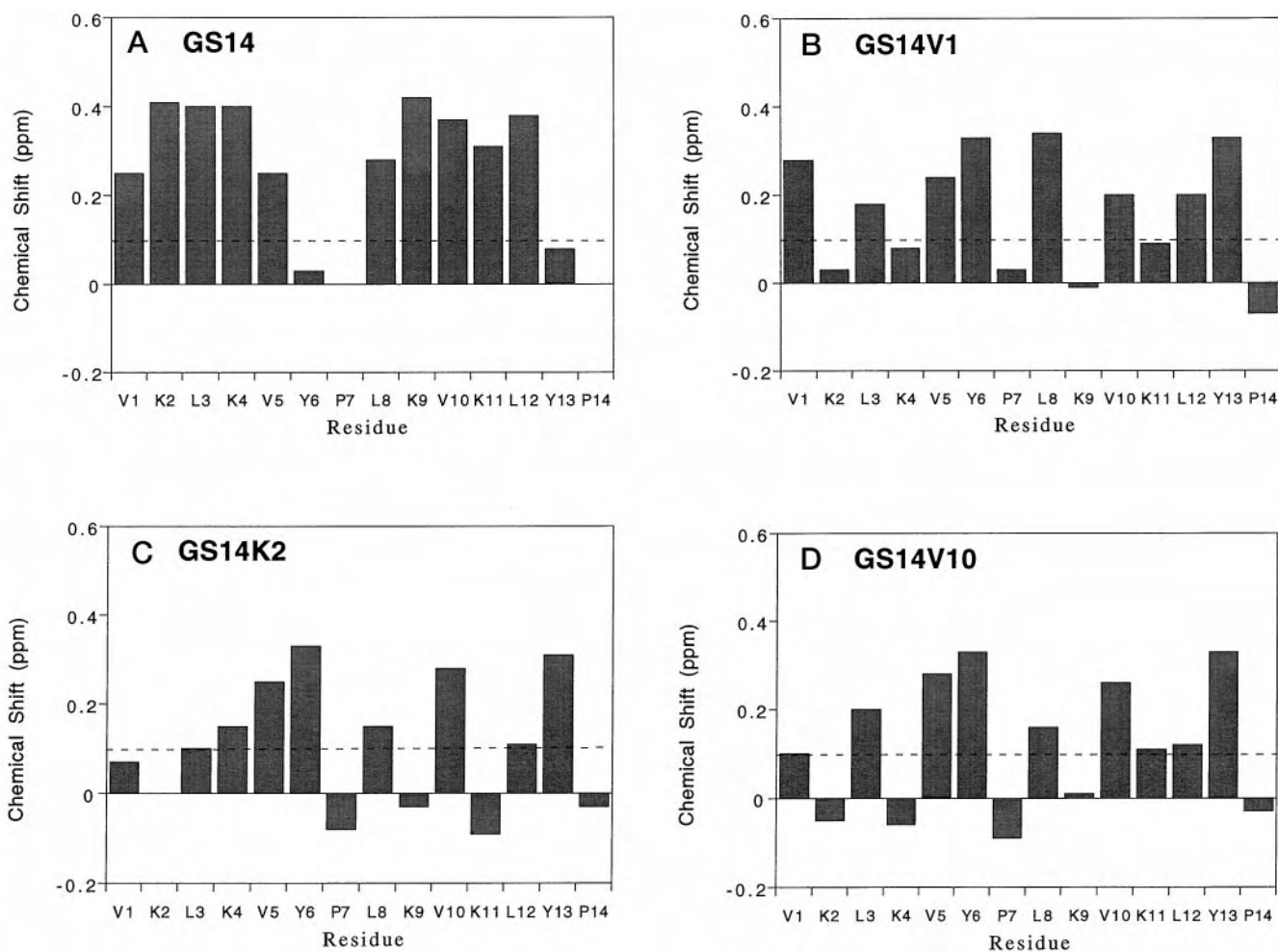
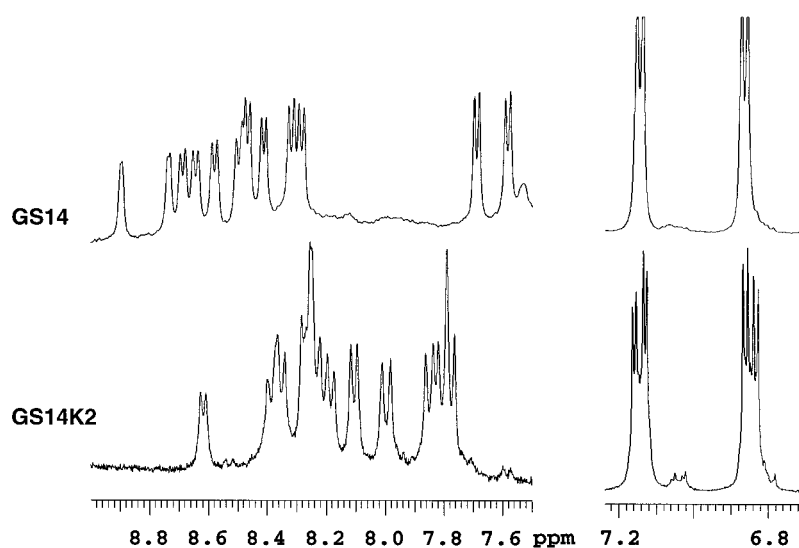


FIG. 4. Chemical shift analysis of GS14 and representative GS14 diastereomers. The chemical shift deviations of  $\alpha$ -proton resonances relative to random coil values are shown for GS14 (A), GS14V1 (B), GS14K2 (C), and GS14V10 (D). Three or more continuous positive chemical shift deviations greater than 0.1 ppm (dashed line) are indicative of  $\beta$ -sheet structure.

potentially six hydrogen bonds that could be formed to stabilize the  $\beta$ -sheet structure of GS14 located between all Val and Leu residues. The non-H-bonded sites are all occupied by Lys residues (Fig. 5, upper panel).

**Reversed-phase HPLC Analysis**—Retention time on reversed-phase HPLC can be used as a measure of peptide hydrophobicity (30, 31). It is well known, however, that the for-

mation of a hydrophobic binding domain due to peptide secondary structure can affect peptide interactions with reversed-phase matrices, this effect having been observed both with  $\alpha$ -helical peptides (32, 33) and  $\beta$ -sheet peptides (21, 34). GS14 and the GS14 diastereomers have exactly the same composition and sequences, and therefore all have the same intrinsic hydrophobicity. Any differences in retention times would be

due to differences in their effective hydrophobicity, which is related to the ability of the peptide to form a hydrophobic preferred binding domain for interaction with the hydrophobic surface of the HPLC matrix. Conversely, the positioning of positive charges in the vicinity of the hydrophobic binding domain would also serve to destabilize the hydrophobic interactions and substantially decrease the overall hydrophobicity of the preferred hydrophobic binding domain (7, 35, 36). Because retention time of the GS14 diastereomers on RP-HPLC is a measure of the ability to form a large hydrophobic binding

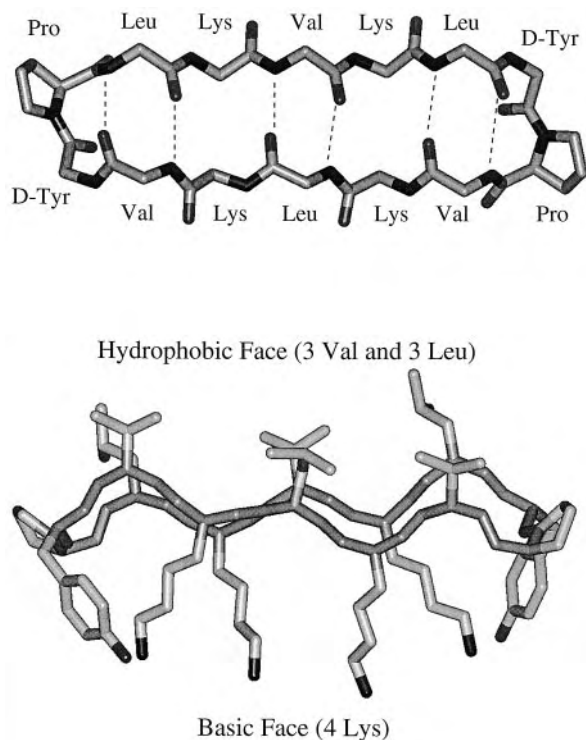


FIG. 5. **Molecular model of GS14.** The model was constructed to contain  $\beta$ -sheet dihedral angles for residues in the strands and two type II'  $\beta$ -turns defined by the Xaa-D-Tyr-Pro-Xaa sequence. An amide bond was formed between the N and C termini, and energy minimization of the structure carried out as described under "Materials and Methods." *Upper panel*, a top view of the backbone of GS14 indicating the positions of potential interstrand hydrogen bonds. *Lower panel*, a side view of GS14 indicating the relative positioning of hydrophobic and basic residues.

domain and at the same time segregate hydrophobic and hydrophilic side chains to opposite sides of the molecule, it is therefore also a measure of amphipathicity in these peptides. The RP-HPLC separation of a mixture of GS14 and the 14 diastereomers is shown in Fig. 6. There was a wide range of retention times observed for the analogs, and all had a lower retention time than GS14. As seen from the model of GS14 (Fig. 5) the parent molecule exists in a highly amphipathic  $\beta$ -sheet conformation with a large hydrophobic preferred binding domain formed by six hydrophobic residues on one face of the molecule, as well as the basic residues sequestered on the opposite face of the molecule. All diastereomers had lower retention times compared with GS14 due to decreased amphipathicity caused by either a decreased size of the hydrophobic preferred binding domain or the relative positioning of hydrophobic and basic residues. Measurement of retention times of the diastereomers on RP-HPLC is therefore a convenient means for ranking and comparing peptide amphipathicity in this homologous series of peptides. The extent of disruption of amphipathicity was dependent on the position of the enantiomeric substitution, with diastereomers containing substitutions in the non-H-bonded sites (Lys in this case) being much more disruptive than those with substitutions in the H-bonded sites (Val and Leu). Enantiomeric substitutions in the center of the  $\beta$ -sheet (Leu<sup>3</sup> and Val<sup>10</sup>) as well as Pro residues in the turns were least disruptive.

#### Membrane Interactions of GS14 Diastereomers

*Interaction with Bacterial Lipopolysaccharide*—Cationic peptides interact with Gram-negative bacteria by initially binding to LPS prior to self-promoted uptake across the outer membrane (37, 38). We investigated the interaction between GS14 diastereomers and the bacterial outer membranes by monitoring the displacement of LPS-bound dansyl-polymyxin B by the peptides (19, 39). The LPS binding affinity of GS14 was extremely strong, approaching that of polymyxin B itself (19), whereas all the diastereomers had lower affinity (Table I). There is a good correlation between binding affinity and retention time on RP-HPLC (Fig. 7), with those peptides having a longer retention time exhibiting higher affinity for LPS. This indicates that the peptides that are more amphipathic (a greater hydrophobicity of the preferred binding domain and therefore also a larger oriented basic face) also bind tighter to LPS. The binding affinity of GS was lower than all the diastereomers, although GS has the greatest retention time on RP-

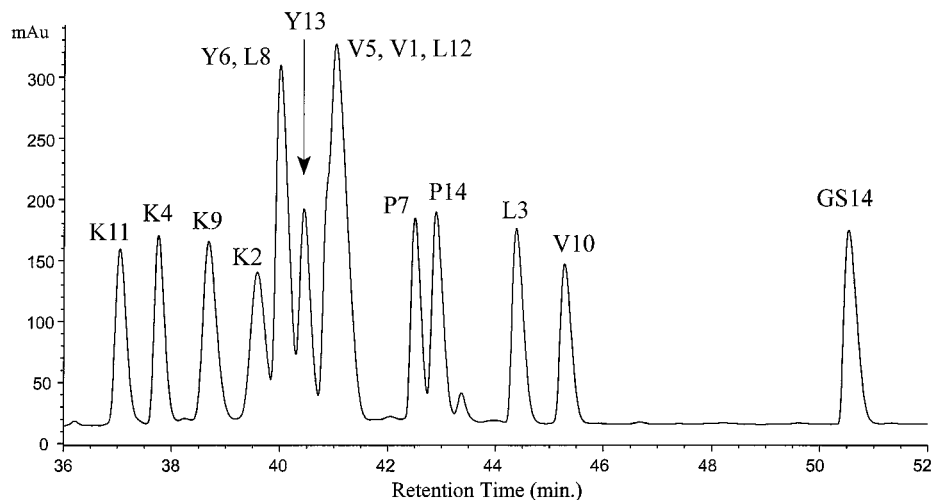


FIG. 6. **RP-HPLC separation of GS14 and single residue substitution diastereomers.** A mixture of GS14 and the 14 diastereomers was separated by RP-HPLC as described under "Materials and Methods." The position of the enantiomeric substitution is shown for each peak on the chromatogram.

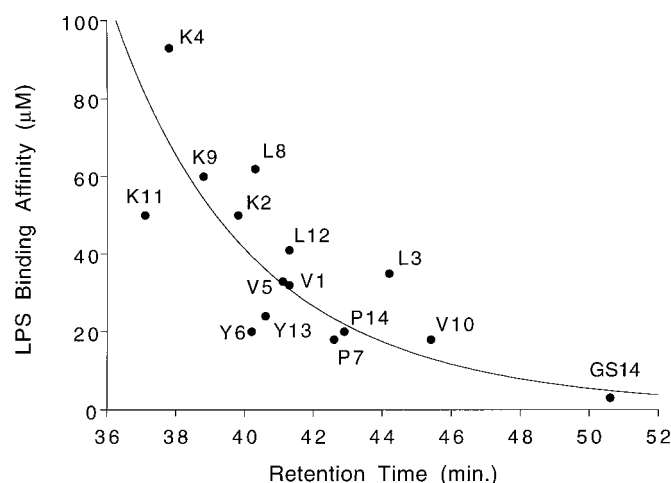


FIG. 7. Correlation between amphipathicity and LPS binding affinity in GS14 diastereomers. Retention times on RP-HPLC were determined for each diastereomer as shown in Fig. 6, and LPS binding affinities as listed in Table I were measured as described under "Materials and Methods." The position of the enantiomeric substitution is shown for each point. The line is drawn to guide the eye.

HPLC (Table I), showing that the increased number of basic residues and size of the molecule (compared with GS) also play a role in binding the outer membranes. These findings are in line with those of a previous study (19) where it was found that both the number of hydrophobic residues and the number of positive charges, as well as their relative positioning, were important in LPS binding.

**Permeabilization of Outer Membranes to NPN**—Permeabilization of *E. coli* outer membranes by GS14 diastereomers was monitored using the hydrophobic fluorescent probe NPN. NPN fluorescence is substantially increased when it is incorporated into the hydrophobic bacterial cell membrane (after permeabilization) compared with its fluorescence in the presence of bacterial cells under non permeabilizing conditions (40). Outer membrane destabilization by representative GS14 diastereomers is shown in Fig. 8. All the diastereomers were found to exhibit essentially similar capacities to permeabilize the outer membrane to the hydrophobic probe at high concentrations; however, at lower concentrations all were more effective than GS14.

#### Structure-Activity Relationships in GS14 Diastereomers

**Hemolytic Activity**—GS14 exhibits extremely high hemolytic activity against human erythrocytes as shown in Table I. The diastereomers exhibited a wide range of activities, ranging from activity similar to GS14 to greatly reduced hemolytic activity. As shown in Fig. 9, there was a clear relationship between amphipathicity and hemolytic activity. Those analogs that were more amphipathic were also more hemolytic. Most significantly, however, in the least hemolytic single substitution diastereomer, GS14K4, hemolytic activity was reduced more than 130-fold compared with the parent GS14. In keeping with this trend, hemolytic activity was further reduced in those diastereomers containing either two or four enantiomeric substitutions due to further decreases in amphipathicity (Table I).

**Gram-negative Antibacterial Activity**—The antimicrobial activity of the diastereomers against a range of Gram-negative microorganisms is shown in Table II. GS14 itself had no activity against any of the microorganisms tested. The majority of diastereomers exhibited at least some activity against most of these microorganisms, with some analogs displaying very strong activity. The therapeutic index of the diastereomers was calculated as a measure of specificity of the peptide for the

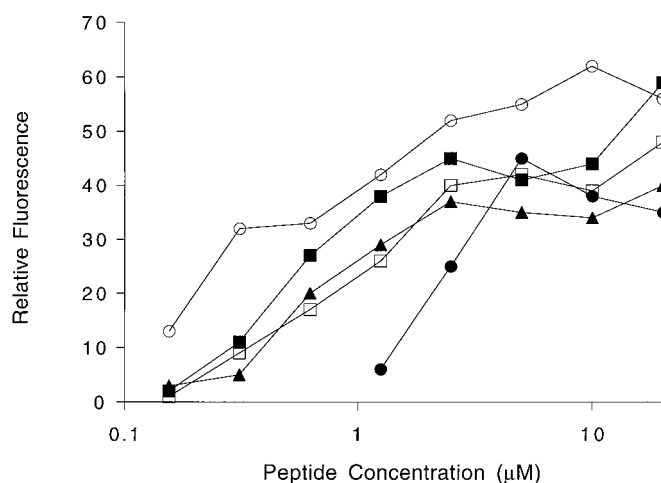


FIG. 8. Permeabilization of *E. coli* UB1005 cells to NPN. Peptide-mediated outer membrane destabilization was monitored by fluorescence increase due to NPN partitioning into the hydrophobic membrane interior. Samples were GS14 (●), GS14V1 (○), GS14K2 (□), GS14K4 (■), and GS14V5 (▲).

microorganism over human erythrocytes (Table II). It is apparent that GS14 has an extremely low therapeutic index, a value of less than 0.01, indicating that it has much greater activity against erythrocytes than Gram-negative microorganisms. The majority of diastereomers exhibited an increase in therapeutic index, with a number of these showing a substantial improvement in specificity (indices greater than 10) representing a greater than 1,000-fold improvement over GS14. The therapeutic indices for GS14 and the two best diastereomers, GS14K4 and GS14K11, are boxed in Table II to highlight the large differences in specificities between these peptides. The best diastereomer, GS14K4, demonstrated a greater than 6,500-fold increase in specificity for two separate microorganisms (*P. aeruginosa* H188 and *E. coli* DC2). The improved therapeutic index reflects both the enhanced antimicrobial activity and the decreased hemolytic activities of the diastereomers. The activity and specificity of GS is also shown in Table II for comparison. The best GS14 diastereomer, GS14K4, exhibited substantially greater specificity than GS for all the Gram-negative microorganisms tested, with therapeutic indices in the range of 13–35-fold greater than GS itself. There was a relationship between both Gram-negative antimicrobial activity and specificity with amphipathicity as shown in Fig. 10. For all microorganisms tested, the antimicrobial activity increased with decreasing retention time on RP-HPLC (decreasing amphipathicity). This, coupled with decreased hemolytic activity in those diastereomers with lower amphipathicity (Fig. 9), resulted in substantial increases in the therapeutic indices compared with GS14. Diastereomers containing either two or four enantiomeric substitutions were generally less active against Gram-negative microorganisms than the best single substitution analogs, but in the case of GS14K2K4, due to decreases in both antimicrobial and hemolytic activities, this analog exhibited a therapeutic index against *E. coli* DC2 similar to those of the two best diastereomers (Table II).

**Gram-positive Antibacterial and Antifungal Activity**—The activity of the diastereomers against Gram-positive microorganisms and yeast is shown in Table III. GS14 was inactive against four of the Gram-positive microorganisms tested but exhibited strong activity against both *Enterococcus faecalis* (MIC 2.3 µg/ml) and *Corynebacterium xerosis* (MIC 6.2 µg/ml). All of the single residue substitution diastereomers also exhibited strong activity against both *E. faecalis* and *C. xerosis*.

TABLE II  
Gram-negative activity and specificity of GS14 diastereomers

Peptide	Minimal Inhibitory Concentration ( $\mu\text{g/ml}$ ) and Therapeutic Index <sup>a</sup>											
	<i>P. aeruginosa</i> H187		<i>P. aeruginosa</i> H188		<i>E. coli</i> UB1005		<i>E. coli</i> DC2		<i>S. typhimurium</i> C587		<i>S. typhimurium</i> C610	
	Activity	Index	Activity	Index	Activity	Index	Activity	Index	Activity	Index	Activity	Index
GS	25	0.5	6.2	2	9	1.4	3.1	4	18	0.7	9	1.4
GS14	>200	<0.01	>200	<0.01	>200	<0.01	>200	<0.01	>200	<0.01	>200	<0.01
GS14V1	60	0.8	3.1	16	6.2	8.1	3.1	16	50	1	6.2	8.1
GS14K2	75	1	6.2	12	12.5	6	3.1	24	25	3	3	25
GS14L3	>200	<0.1	200	0.1	200	0.1	50	0.25	>200	<0.1	>200	<0.1
GS14K4	25	8	3.1	65	6.2	32	3.1	65	12.5	16	4	50
GS14V5	100	1.5	6.2	24	15	10	3.1	48	100	1.5	12.5	12
GS14Y6	200	0.1	50	0.5	50	0.5	3.1	8.1	>200	<0.1	100	0.25
GS14P7	200	0.06	100	0.1	200	0.06	6.2	2	>200	<0.06	200	0.06
GS14L8	37	1.4	3.1	16	6.2	8.1	3.1	16	12.5	4	6.2	8.1
GS14K9	50	2	6.2	16	12.5	8	3.1	32	17	5.9	6.2	16.1
GS14V10	>200	<0.03	200	0.03	200	0.03	3.1	2	>200	<0.03	200	0.03
GS14K11	37	4.1	5	30	6.2	24	3.1	48	12.5	12	6.2	24
GS14L12	200	0.2	12.5	2.8	17	2.1	3.1	11	150	0.2	50	0.7
GS14Y13	>200	<0.06	100	0.1	100	0.1	3.1	4	>200	<0.06	>200	<0.06
GS14P14	>200	<0.05	100	0.1	100	0.1	4	2.3	>200	<0.05	>200	<0.05
GS14K2K4	150	2.7	12.5	32	50	8	6.2	65	200	2	25	16
GS14K2K4K9K11	>200	- <sup>b</sup>	12.5	>64	100	>8	50	>16	>200	-	25	>32

<sup>a</sup> Therapeutic index = hemolytic activity/antimicrobial activity. For calculation of the therapeutic index, values of 400  $\mu\text{g/ml}$  were used for MIC values of >200  $\mu\text{g/ml}$ , and values of 1600  $\mu\text{g/ml}$  were used for hemolytic activity values of >800  $\mu\text{g/ml}$  (Table I). The therapeutic indices of GS14 and the two best diastereomers are boxed.

<sup>b</sup> Therapeutic index could not be calculated.

However, they also displayed strong activity against *Staphylococcus epidermidis* and moderate activity against the remainder of the Gram-positive microorganisms tested. GS14 was essentially inactive against the yeast *Candida albicans*, but all of the diastereomers exhibited antifungal activity ranging from moderate to strong. Coupled with the decreased hemolytic activity of the diastereomers, there was again a large increase in therapeutic indices relative to GS14 for all of these microorganisms. Increases in selectivity over GS14 were in the order of 200-fold for *E. faecalis*, 1,000-fold for *C. xerosis*, 3,000-fold for *C. albicans*, and 10,000-fold for *S. epidermidis* for the best diastereomers (GS14K4 and GS14K11). The therapeutic indices for GS14 and the best diastereomers are boxed in Table III to highlight these differences. As for Gram-negative microorganisms, there was a relationship between amphipathicity and Gram-positive activity, antifungal activity, and specificity (Fig. 11). For those microorganisms against which GS14 exhibited activity (*E. faecalis* and *C. xerosis*), the activities remained relatively constant in all the analogs, but the therapeutic indices were increased due to a reduction in hemolytic activity. For the remainder of the microorganisms against which GS14 was inactive, there was an increase in both activity and therapeutic index with decreasing amphipathicity. The most active diastereomers displayed activities that were essentially equal to GS itself for three of the Gram-positive microorganisms and yeast but with therapeutic indices in the order of 10-fold higher than GS, due primarily to reduced hemolytic activity. However, for three other microorganisms, which included two *Staphylococcus aureus* strains and *Bacillus subtilis*, the best diastereomers were approximately 10-fold less active than GS, although the therapeutic indices were comparable.

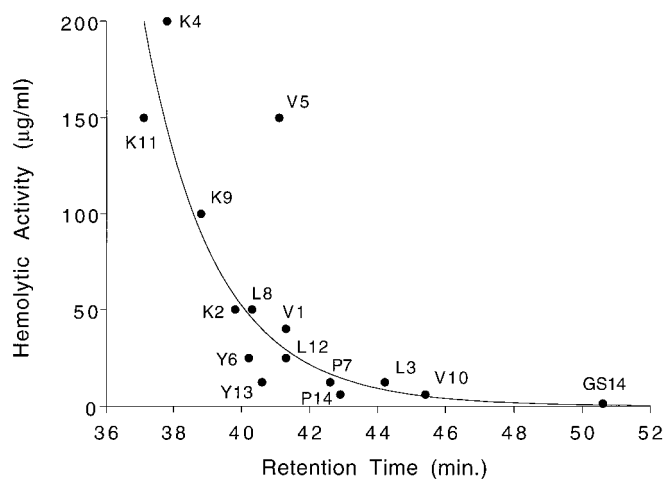


FIG. 9. Correlation between amphipathicity and hemolytic activity in GS14 diastereomers. Retention times on RP-HPLC were determined for each diastereomer as shown in Fig. 6, and hemolytic activity as listed in Table I was measured as described under "Materials and Methods." The line is drawn to guide the eye.

#### DISCUSSION

The role of amphipathicity (polarization of hydrophobicity and positive charge) in antimicrobial and hemolytic activities of a series of homologous cyclic peptides was investigated in this study. All the GS14 analogs had exactly the same composition and sequence and therefore shared similar intrinsic physicochemical properties (basicity and hydrophobicity). Our findings show that enantiomeric substitutions within the framework of GS14 were responsible for the disruption of both the  $\beta$ -sheet

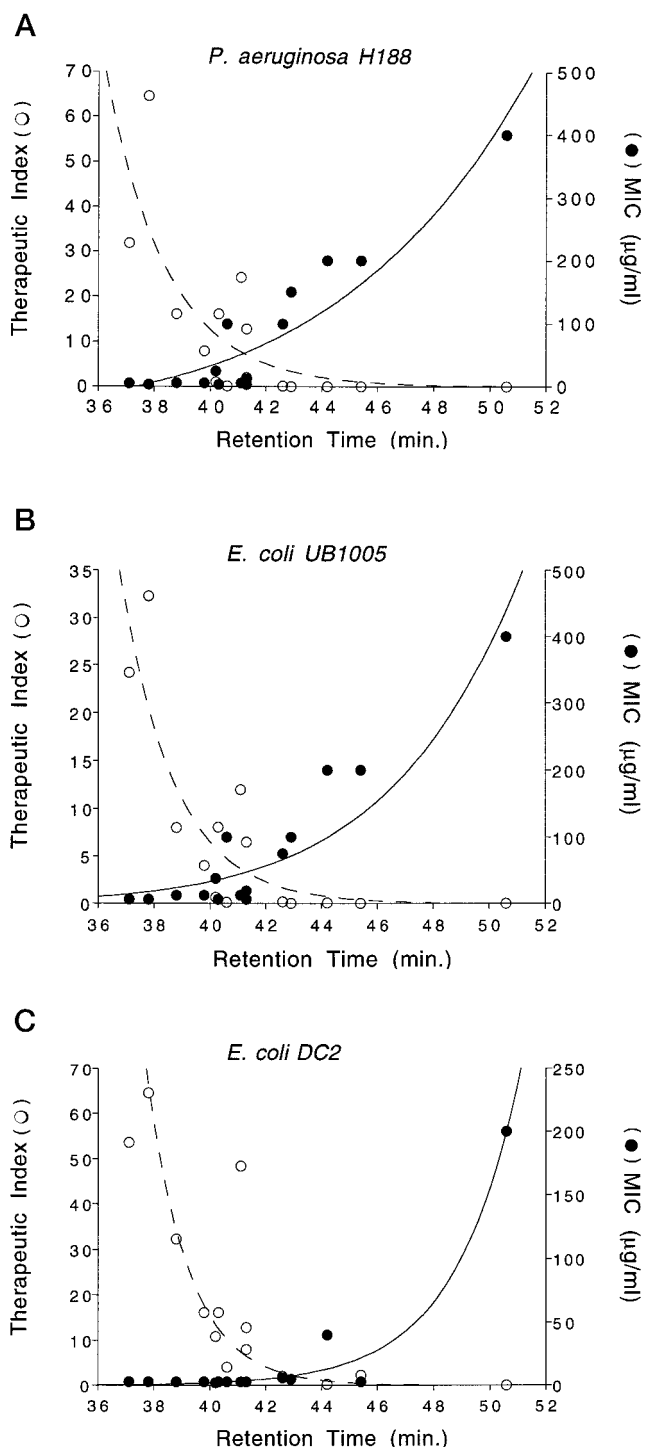


FIG. 10. Antimicrobial activity and microbial specificity of GS14 diastereomers against Gram-negative microorganisms. The minimal inhibitory concentration (●) and therapeutic index (○) of the single residue enantiomeric substitution analogs shown in Table II are plotted as a function of retention time on RP-HPLC. Plots are for *P. aeruginosa* H188 (A), *E. coli* UB1005 (B), and *E. coli* DC2 (C). MIC values of >200 µg/ml are plotted as 400 µg/ml. The lines are drawn to guide the eye.

structure and amphipathicity in the diastereomers. However, all sites were not equivalent in that each substitution resulted in a unique amount of perturbation of amphipathicity, depending on the substitution position. Enantiomeric substitutions in the non-H-bonded sites of GS14 (Lys residues) resulted in the greatest disruption of amphipathicity. Molecular modelling studies utilizing the  $\beta$ -sheet backbone structure of GS14 have

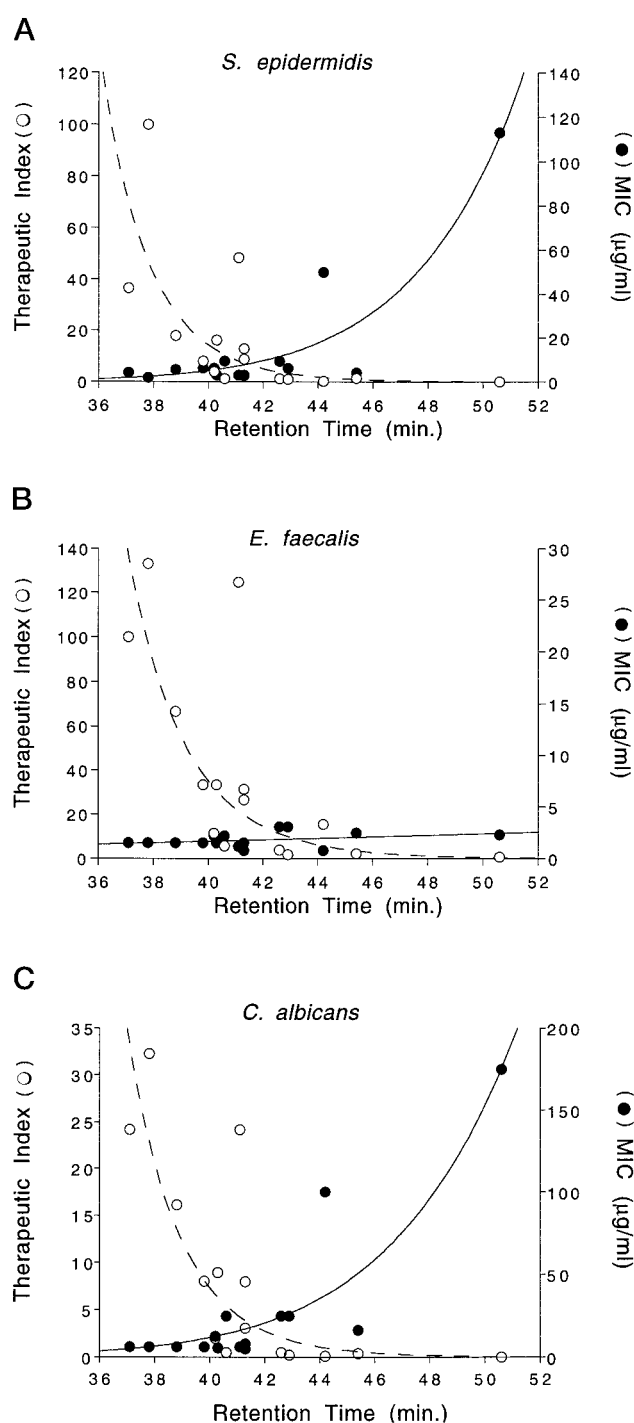


FIG. 11. Antimicrobial activity and microbial specificity of GS14 diastereomers against Gram-positive microorganisms and yeast. The minimal inhibitory concentration (●) and therapeutic index (○) of the single residue enantiomeric substitution analogs shown in Table III are plotted as a function of retention time on RP-HPLC. Plots are for *S. epidermidis* (A), *E. faecalis* (B), and *C. albicans* (C). The lines are drawn to guide the eye.

shown that enantiomeric substitutions at positions corresponding to the Lys residues result in the positioning of the positively charged side chains closer to the hydrophobic face of the molecule, whereas substitutions in the H-bonded sites result in repositioning of the hydrophobic side chain on the same face of the molecule (data not shown). Similar effects have been noted with amphipathic helices where substitution of basic residues on the hydrophobic face of the helix had a greater effect on

TABLE III  
 Antifungal and Gram-positive activity and specificity of GS14 diastereomers

Peptide	Minimal Inhibitory Concentration ( $\mu\text{g/ml}$ ) and Therapeutic Index <sup>a</sup>													
	<i>S. aureus</i> SAP0017		<i>S. aureus</i> K147		<i>S. epidermidis</i>		<i>B. subtilis</i>		<i>E. faecalis</i>		<i>C. xerosis</i>		<i>C. albicans</i>	
	Activity	Index	Activity	Index	Activity	Index	Activity	Index	Activity	Index	Activity	Index	Activity	Index
GS	1.5	8.3	1.5	8.3	1.5	8.3	3.1	4	3.1	4	0.8	16	4	3.1
GS14	>200	<0.01	>200	<0.01	200	0.01	>200	<0.01	1.5	1	9	0.2	150	0.01
GS14V1	50	1	100	0.5	3.1	16	50	1	1.5	33	1.5	33	5	10
GS14K2	50	1.5	100	0.8	6.2	12	50	1.5	1.5	50	0.8	94	6.2	12
GS14L3	200	0.06	>200	<0.06	50	0.25	>200	<0.06	0.8	16	0.8	16	100	0.1
GS14K4	50	4	100	2	2	100	25	8	1.5	133	1.5	133	6.2	32
GS14V5	50	3	100	1.5	3.1	48	200	0.8	1.5	100	1.5	100	6.2	24
GS14Y6	>200	<0.1	>200	<0.1	6.2	4	>200	<0.1	3.1	8.1	1	25	12.5	2
GS14P7	>200	<0.06	>200	<0.06	6.2	2	>200	<0.06	6.2	2	1	12.5	25	0.5
GS14L8	25	2	50	1	3.1	16	12.5	4	1.5	33	0.8	63	6.2	8
GS14K9	25	4	50	2	6.2	16	25	4	1.5	67	1.5	67	6.2	16
GS14V10	50	0.1	200	0.03	3.1	2	200	0.03	1.5	4	0.8	8	17	0.4
GS14K11	25	6	25	6	3.1	48	25	6	1.5	100	0.8	188	6.2	24
GS14L12	50	0.7	100	0.4	3.1	11	200	0.2	0.8	44	3.1	11	9	3.9
GS14Y13	>200	<0.06	>200	<0.06	9	1.4	>200	<0.06	3.1	4	1	12.5	25	0.5
GS14P14	>200	<0.1	>200	<0.1	6.2	1.5	>200	<0.01	6.2	1.5	1	9	25	0.4
GS14K2K4	>200	<2	>200	<2	100	4	>200	<2	>200	<2	9	44	200	2
GS14K2K4K9K11	>200	- <sup>b</sup>	>200	-	>200	-	>200	-	>200	-	25	>32	>200	-

<sup>a</sup> Therapeutic index = hemolytic activity/antibacterial activity. For calculation of the therapeutic index, values of 400  $\mu\text{g/ml}$  were used for MIC values of >200  $\mu\text{g/ml}$ , and values of 1600  $\mu\text{g/ml}$  were used for hemolytic activity values of >800  $\mu\text{g/ml}$  (Table 1). The therapeutic indices of GS14 and the two best diastereomers are boxed.

<sup>b</sup> Therapeutic index could not be calculated.

amphipathicity than hydrophobic substitutions on the hydrophilic face, which have little effect on the hydrophobicity of the preferred hydrophobic binding domain (7, 35, 36, 41). The GS14 diastereomers were found to undergo changes in backbone conformation in hydrophobic lipid-mimicking environments, similar to that seen with linear nonconstrained peptides. However, due to the constrained nature of the cyclic peptides, these conformational changes would be expected to be relatively small compared with linear peptides.

The observed amphipathicities of the diastereomers correlated well with their hemolytic properties, showing that hemolytic activity is driven by high amphipathicity, and more likely, the presence of a large hydrophobic face. Analogous findings were reported in a previous study on GS-like cyclic 10 residue peptides in which  $\beta$ -sheet structure and the basic face were retained, but only hydrophobic residues were altered (16). The fact that GS itself has high hemolytic activity, although approximately 10-fold less than GS14, again supports this conclusion, because GS also has an amphipathic nature with a large hydrophobic face, albeit smaller than GS14. We assume that the presentation of a large hydrophobic face promotes the partitioning into membranes of any cell, whereas partitioning into bacterial membranes, which tend to carry strong negative charges and have a large (internal negative) electrical potential gradient, is further promoted by the cationic charge of these GS peptides. Our findings indicate that in the context of GS-like cyclic peptides, hemolytic activity can be reduced either through reduction of amphipathicity (to reduce the "directed hydrophobicity" of the hydrophobic domain) as well as by reduction of overall peptide hydrophobicity. Both these design elements can be incorporated into peptides either through sequence or structural (*e.g.* enantiomeric substitutions and ring size) manipulation. Similar findings associating increased hydrophobicity or amphipathicity with increased hemolytic activity have also been reported for nonconstrained linear peptides (6–8, 42). Modulation of amphipathicity and hydrophobicity

therefore appears to be a generally applicable method of regulating hemolytic activity in antimicrobial peptides of different structural classes.

The antimicrobial activity of the GS14 diastereomers against Gram-negative microorganisms was found to increase with decreasing amphipathicity. This is likely a reflection of the higher binding affinity for outer membrane components by analogs with high amphipathicity (Fig. 7). These high affinity interactions would be expected to decrease the ability of the peptides to penetrate to and accumulate at their site of action on the inner membrane. All diastereomers were found to have similar capacities to destabilize the outer membrane following binding. It would therefore appear that binding to outer membrane components, regardless of the affinity, is sufficient to destabilize the outer membrane, but only those peptides with appropriate binding affinity can easily penetrate to the inner membrane. There was a similar trend of increasing Gram-positive antimicrobial activity with decreasing amphipathicity in the diastereomers. Although these microorganisms have no outer membrane, they possess a peptidoglycan layer that contains negatively charged groups from teichoic acid as well as from the amino acids composing the peptidoglycan layer. It is possible that a similar mechanism may be responsible for the decreased antimicrobial activity by highly amphipathic diastereomers whereby binding to peptidoglycan components results in decreased accumulation of the peptides in the cytoplasmic membrane. Unlike GS14 and the diastereomers, GS exhibited strong antimicrobial activity against all the microorganisms tested. These differences may again be related to outer membrane binding because GS was found to have approximately 100-fold lower affinity for LPS compared with GS14.

Our findings relating increased amphipathicity with decreased antimicrobial activity in the present cyclic peptides are in agreement with a previous study by Blondelle and Houghten (7), who utilized model linear  $\alpha$ -helical peptides. In contrast, two recent studies by Bienert and co-workers (6, 11) also uti-

lizing linear  $\alpha$ -helical peptides reported an opposite trend in which antimicrobial activity either remained relatively constant or decreased with decreasing amphipathicity. Differences in overall peptide hydrophobic moments (quantitated amphipathicity,  $\mu$ ), however, may explain these discrepancies. GS14 has a high hydrophobic moment ( $\mu = 0.531$ ) that is essentially equivalent to those linear  $\alpha$ -helical peptides (7), which exhibited similar trends in antimicrobial activity ( $\mu = 0.521$ ). In contrast, the linear  $\alpha$ -helical peptides that exhibited the opposite trends had substantially lower hydrophobic moments ( $\mu = 0.284$  to  $0.451$  and  $\mu = 0.329$  to  $0.391$  (Ref. 6);  $\mu = 0.334$  (Ref. 11)). It is possible that the differences in the observed activities between these sets of peptides is related to their overall amphipathicity and its influence on peptide outer membrane interactions. As shown in the present study, highly amphipathic molecules bind to outer membrane components with a greater affinity compared with those with decreased amphipathicity, which apparently results in decreased antimicrobial activity (presumably by impeding the subsequent movement of the peptide toward its internal targets or by interfering with co-operativity that is essential for trans-outer membrane uptake). Thus, increased outer membrane interactions by the more amphipathic linear  $\alpha$ -helical peptides (7) may explain the similar trend as seen with the highly amphipathic GS14 peptides. It is possible that the  $\alpha$ -helical peptides with decreased amphipathicity (6, 11) were of low enough amphipathicity that these outer membrane interactions were reduced. In support of this, we also found in the present study that decreasing the amphipathicity past a certain threshold resulted in a trend of decreasing antimicrobial activity similar to that observed with the less amphipathic  $\alpha$ -helical peptides (6, 11). One may also speculate that peptide outer membrane interactions between the present cyclic peptides and linear peptides may also differ. The greater conformational entropy upon binding of linear peptides would be expected to result in decreased binding affinity to outer membrane or peptidoglycan components compared with the present constrained peptides, thereby facilitating the partitioning of those peptides to the inner membrane. Linear peptides would also tend to cover a larger surface area, which may also influence their action on outer membranes.

As mentioned above, we found that there was a threshold amphipathicity required for antimicrobial activity below which activity decreased as exemplified by those diastereomers containing either two or four enantiomeric substitutions. We have also previously found that linear nonconstrained peptides related to GS are inactive (16). Both these observations support the concept that there is a minimum amphipathicity or minimum size of the hydrophobic domain required for antimicrobial activity in these cyclic peptides. Although the actual mechanism of lipid membrane disruption by these peptides is not known, there is evidence suggesting that the formation of nonlamellar phases are a feature of their mode of action (43). The formation of such phases would presumably require a certain proportion of the molecule to partition into the hydrophobic portion of the membrane to result in such a rearrangement of membrane architecture. One would therefore expect that there be a minimum size of a hydrophobic domain required to allow partitioning of a critical portion of the peptide into the membrane. Similar to the antimicrobial activity, hemolytic activity also decreased with decreasing amphipathicity. We were, however, able to identify an optimum amphipathicity where the therapeutic index was maximum in the present diastereomers. The fact that complete specificity was not achieved in the present cyclic peptides by modulation of amphipathicity may be a reflection that the proposed site of action of these peptides are biological membranes. Although there are differences between

prokaryotic and eukaryotic membrane composition, these differences may not be large enough to obtain complete specificity in these antimicrobial peptides, but rather, the therapeutic indices can be optimized to provide the greatest discrimination. Similarly, because there are species to species variations in both cytoplasmic lipid as well as outer membrane compositions, it is possible that there will be different optimal peptide properties for different species.

In summary, we have shown that a preformed highly amphipathic nature is not desirable in the present cyclic peptides because this results in decreased specificity as well as increased interactions with outer membrane components. By systematic manipulation of the amphipathicity of GS14, it was possible to identify peptides possessing optimal amphipathicities leading to the highest therapeutic indices. These cyclic peptides and likely other constrained peptides appear to share similar requirements for activity and specificity as the linear unconstrained antimicrobial peptides. However, our findings also suggest that outer membrane interactions may play a significant role in the observed antimicrobial properties of antimicrobial peptides in general and further that these interactions may be of greater importance for conformationally restricted molecules. We are currently utilizing the best structural framework (amphipathicity) derived from the present study to investigate the role of intrinsic hydrophobicity as well as basicity to further optimize the therapeutic indices of these cyclic peptides. The three-dimensional structures of the present peptides in aqueous medium and in lipid environments are also being determined by NMR spectroscopy, and in-depth lipid binding/disruption studies are currently in progress. Knowledge of both structure and mechanism will ultimately allow us to design peptides possessing the greatest activity and specificity.

**Acknowledgments**—We thank Paul Semchuk, Leonard Daniels, and Marc Genest for assistance with peptide synthesis and purification and Bob Luty for CD measurements. We also thank Pierre Lavigne for helpful discussions and Campbell McInnes for preparation of supplementary material.

#### REFERENCES

1. Travis, J. (1994) *Science* **264**, 360–362
2. Hancock, R. E. W. (1997) *Lancet* **349**, 418–422
3. Hancock, R. E. W., and Lehrer, R. (1998) *Trends Biotechnol.* **16**, 82–88
4. Pathak, N., Salas-Auvert, R., Ruche, G., Janna, M.-H., McCarthy, D., and Harrison, R. G. (1995) *Proteins Struct. Funct. Genet.* **22**, 182–186
5. Izumiya, N., Kato, T., Aoyaga, H., Waki, M., and Kondo, M. (1979) *Synthetic Aspects of Biologically Active Cyclic Peptides: Gramicidin S and Tyrocidines*, pp. 49–89, Halsted Press, New York
6. Dathe, M., Wieprecht, T., Nikolenko, H., Handel, L., Maloy, W. L., MacDonald, K., Beyermann, M., and Bienert, M. (1997) *FEBS Lett.* **403**, 208–212
7. Blondelle, S. E., and Houghten, R. A. (1992) *Biochemistry* **31**, 12688–12694
8. Oren, Z., Hong, J., and Shai, Y. (1997) *J. Biol. Chem.* **272**, 14643–14649
9. Shai, Y., and Oren, Z. (1996) *J. Biol. Chem.* **271**, 7305–7308
10. Oren, Z., and Shai, Y. (1997) *Biochemistry* **36**, 1826–1835
11. Dathe, M., Shumann, M., Wieprecht, T., Winkler, A., Beyermann, M., Krause, E., Matsuzaki, K., Murase, O., and Bienert, M. (1996) *Biochemistry* **35**, 12612–12622
12. Gause, G. F., and Brazhnikova, M. G. (1944) *Nature* **154**, 703
13. Rackovsky, S., and Scheraga, H. A. (1980) *Proc. Natl. Acad. Sci. U. S. A.* **77**, 6965–6967
14. Hull, S. E., Karlsson, R., Main, P., and Woolfson, M. M. (1978) *Nature* **275**, 206–207
15. Ovchinnikov, Y. A., and Ivanov, V. T. (1975) *Tetrahedron* **31**, 2177–2209
16. Kondejewski, L. H., Farmer, S. W., Wishart, D. S., Hancock, R. E. W., and Hodges, R. S. (1996) *Int. J. Peptide Protein Res.* **47**, 460–466
17. Katayama, T., Nakao, K., Akamatsu, M., Ueno, T., and Fumita, T. (1994) *J. Pharmacol. Sci.* **83**, 1357–1362
18. Tamaki, M., Takimoto, M., Nozaki, S., and Muramatsu, I. (1987) *J. Chrom. Biomed. Appl.* **413**, 287–292
19. Kondejewski, L. H., Farmer, S. W., Wishart, D. S., Kay, C. M., Hancock, R. E. W., and Hodges, R. S. (1996) *J. Biol. Chem.* **271**, 25261–25268
20. Gibbs, A. C., Kondejewski, L. H., Gronwald, W., Nip, A. M., Hodges, R. S., and Wishart, D. S. (1998) *Nat. Struct. Biol.* **5**, 284–288
21. Wishart, D. S., Kondejewski, L. H., Semchuk, P. D., Sykes, B. D., and Hodges, R. S. (1996) *Letters Peptide Sci.* **3**, 53–60
22. Wishart, D. S., Sykes, B. D., and Richards, F. M. (1992) *Biochemistry* **31**, 1647–1651
23. Creighton, T. E. (1984) *Proteins*, pp. 171–237, W. H. Freeman and Company,

- New York
24. Dauber-Ogusthorpe, P., Roberts, V. A., Ogusthorpe, D. J., Wolff, J., Genest, M., and Hagler, A. T. (1988) *Proteins Struct. Funct. Genet.* **4**, 31–37
  25. Eisenberg, D., Schwarz, E., Komaromy, M., and Wall, R. (1984) *J. Mol. Biol.* **179**, 125–142
  26. Woody, R. W. (1995) *Methods Enzymol.* **246**, 34–71
  27. Sonnichsen, F. D., Van Eyk, J. E., Hodges, R. S., and Sykes, B. D. (1992) *Biochemistry* **31**, 8790–8798
  28. Blanco, F. J., Jimenez, M. A., Pineda, A., Rico, M., Santoro, J., and Nietol, J. L. (1994) *Biochemistry* **33**, 6004–6014
  29. Cagas, P. M., and Corden, J. L. (1995) *Proteins Struct. Funct. Genet.* **21**, 141–160
  30. Parker, J. M. R., Guo, D., and Hodges, R. S. (1986) *Biochemistry* **25**, 5425–5432
  31. Guo, D., Mant, C. T., Taneja, A. K., Parker, J. M. R., and Hodges, R. S. (1986) *J. Chromatogr.* **359**, 499–517
  32. Zhou, N. E., Mant, C. T., and Hodges, R. S. (1990) *Peptide Res.* **3**, 8–20
  33. Rothemund, S., Krause, E., Beyermann, M., Dathe, M., Bienert, M., Hodges, R. S., Sykes, B. D., and Sonnichsen, F. D. (1996) *Peptide Res.* **9**, 79–87
  34. Krause, E., Beyermann, M., Fabian, H., Dathe, M., Rothemund, S., and Bienert, M. (1996) *Int. J. Peptide Protein Res.* **48**, 559–568
  35. Monera, O. D., Sereda, T. J., Zhou, N. E., Kay, C. M., and Hodges, R. S. (1995) *J. Peptide Sci.* **1**, 319–329
  36. Sereda, T. J., Mant, C. T., Sonnichsen, F. D., and Hodges, R. S. (1994) *J. Chromatogr.* **676**, 139–153
  37. Hancock, R. E. W. (1981) *Antimicrob. Chemother.* **8**, 429–445
  38. Nicas, T. I., and Hancock, R. E. W. (1983) *J. Gen. Microbiol.* **129**, 509–517
  39. Moore, R. A., Bates, N. C., and Hancock, R. E. W. (1986) *Antimicrob. Agents Chemother.* **29**, 496–500
  40. Loh, B., Grant, C., and Hancock, R. E. W. (1984) *Antimicrob. Agents Chemother.* **26**, 546–551
  41. Mant, C. T., Litowski, J. R., and Hodges, R. S. (1998) *J. Chromatogr.* **816**, 65–78
  42. Wieprecht, T., Dathe, M., Beyermann, M., Krause, E., Maloy, W. L., MacDonald, D. L., and Bienert, M. (1997) *Biochemistry* **36**, 6124–6132
  43. Prenner, E. J., Lewis, R. N. A. H., Neuman, K. C., Gruner, S. M., Kondejewski, L. H., Hodges, R. S., and McElhaney, R. N. (1997) *Biochemistry* **36**, 7906–7916